Experimental Dynamic Substructuring: Significance and Perspectives

Walter D'Ambrogio[1][0000−0002−2712−8886] and
Annalisa Fregolent[2][0000−0003−2313−7715]

[1] Università degli Studi dell'Aquila, DIIIE, Piazzale E. Pontieri 1, Monteluco di Roio, 67100 L'Aquila, Italy walter.dambrogio@univaq.it
[2] Università degli Studi di Roma La Sapienza, DIMA, Via Eudossiana 18, 00184 Roma, Italy annalisa.fregolent@uniroma1.it

Abstract. Dynamic substructuring allows to describe an assembled structural system in terms of component subsystems. In experimental dynamic substructuring, the model of at least one (sub)system derives from experimental tests: this allows to consider systems that may be too difficult to model. The degrees of freedom (DoFs) of the assembled system can be partitioned into internal DoFs (not belonging to the couplings) and coupling DoFs. A possible application of experimental dynamic substructuring is substructure decoupling, i.e. the identification of the dynamic model of a structural subsystem embedded in a structural system known from experiments (assembled system) and connected to the rest of the system (residual subsystem) through a set of coupling DoFs. Coupling DoFs are often difficult to observe, either because they cannot be easily accessed or because they include rotational DoFs. However, whilst coupling DoFs and in particular rotational DoFs are needed when coupling together different subsystems, they are not essential in substructure decoupling, because the actions exchanged through the coupling DoFs are already included in the dynamic response of the assembled system. The most promising fields in substructure coupling are: coupling with configuration dependent interface and nonlinear coupling with localized nonlinearities. With reference to substructure decoupling, the most remarkable topics are: interface optimization, configuration dependent coupling conditions, and joint identification.

Keywords: Experimental Dynamic Substructuring · Substructure Decoupling · Interface DoFs

1 Introduction

In the framework of dynamic substructuring, substructure coupling consists in the identification of the dynamic behavior of an assembled structural system, starting from the dynamic behavior of the component subsystems. The degrees of freedom (DoFs) of the assembled system can be partitioned into internal DoFs (not belonging to the couplings) and coupling DoFs. Many well-established techniques exist to perform substructure coupling when all substructures are modeled

theoretically, see for instance [12, 8, 18] and subsequent literature. However, in many cases, the model of at least one subsystem derives from experimental tests, mainly because complex subsystems may be too difficult to model. In this case, one speaks of experimental dynamic substructuring.

A general framework for dynamic substructuring is provided in [15], where primal and dual assembly are introduced. Furthermore, coupling can be performed in the physical domain, in the frequency domain (Frequency Based Substructuring), or in reduced domains (e.g. the modal domain). When using the modal domain or other reduced domains, truncation problems may arise. In Frequency Based Substructuring, Frequency Response Functions (FRFs) are used to avoid modal truncation problems.

A well known issue in experimental substructure coupling is related to rotational DoFs. Whenever coupling DoFs include rotational DoFs, the related rotational FRFs must be obtained experimentally. This becomes a quite complicated task when measuring only translational FRFs, as shown in [20]. Several techniques for measuring rotational responses have been devised, see e.g. [21, 1].

Substructure decoupling represents another possible application of experimental dynamic substructuring. It can be defined as the identification of the dynamic model of a structural subsystem embedded in a structural system known from experiments (assembled system) and connected to the remaining part of the system (residual subsystem) through a set of coupling DoFs. Decoupling is a need for subsystems that cannot be measured separately, but only when coupled to their neighboring substructure(s) (e.g. fixtures needed for testing or subsystems in operational conditions).

Coupling DoFs are often difficult to observe, either because they are not easy to access or because they include rotational DoFs. However, whilst coupling DoFs and in particular rotational DoFs are needed when coupling together different subsystems, they are not essential in substructure decoupling [9]. In fact, the actions exchanged through the connecting DoFs are already embedded in the dynamic response of the assembled system.

Contact problems can also be tackled using a numerical computation technique based on dynamic substructuring, if time varying coupling conditions are assumed. In [6, 2] a sliding contact interface between a rigid suspended bar and a lumped mass is considered, without and with friction. In [3, 7] a sliding contact interface between a horizontal and an oblique cantilever beam is considered, without and with friction, using a basic contact assumption, in order to deal with friction induced vibrations not involving instabilities. In [4, 5] the sliding contact between a horizontal and an oblique cantilever beam is considered again, using more realistic contact assumptions that take into account the deformation of the contacting bodies in order to analyze friction induced instabilities.

In the present contribution, section 2 describes the recent advances of research on experimental substructure coupling, focusing on configuration dependent Frequency Response Function; section 3 deals with substructure decoupling, focusing on interface optimization; finally, section 4 discusses the future perspectives of experimental dynamic substructuring.

2 Experimental Substructure Coupling

Let us consider a dynamic system made up of n coupled subsystems. Each subsystem can be described either in the physical domain using mass, stiffness and damping matrices or in the frequency domain using the dynamic stiffness matrix.

2.1 Frequency Based Substructuring

In the frequency domain, the equation of motion of a linear time-invariant subsystem r may be written as:

$$\mathbf{Z}^{(r)}(\omega)\boldsymbol{u}^{(r)}(\omega) = \boldsymbol{f}^{(r)}(\omega) + \boldsymbol{g}^{(r)}(\omega) \tag{1}$$

where:

$\mathbf{Z}^{(r)}$: dynamic stiffness matrix of subsystem r;
$\boldsymbol{u}^{(r)}$: vector of degrees of displacements of subsystem r;
$\boldsymbol{f}^{(r)}$: vector of external forces on subsystem r;
$\boldsymbol{g}^{(r)}$: vector of connecting forces with other subsystems (internal constraints).

The equation of motion of the n subsystems to be coupled can be written in a block diagonal format, by omitting the frequency dependence:

$$\mathbf{Z}\boldsymbol{u} = \boldsymbol{f} + \boldsymbol{g} \tag{2}$$

with

$$\mathbf{Z} = \begin{bmatrix} \mathbf{Z}^{(1)} & & \\ & \ddots & \\ & & \mathbf{Z}^{(n)} \end{bmatrix}, \quad \boldsymbol{u} = \begin{Bmatrix} \boldsymbol{u}^{(1)} \\ \vdots \\ \boldsymbol{u}^{(n)} \end{Bmatrix}, \quad \boldsymbol{f} = \begin{Bmatrix} \boldsymbol{f}^{(1)} \\ \vdots \\ \boldsymbol{f}^{(n)} \end{Bmatrix}, \quad \boldsymbol{g} = \begin{Bmatrix} \boldsymbol{g}^{(1)} \\ \vdots \\ \boldsymbol{g}^{(n)} \end{Bmatrix}$$

The compatibility condition at the interface DoFs implies that any pair of matching DoFs $u_l^{(r)}$ and $u_m^{(s)}$, i.e. DoF l on subsystem r and DoF m on subsystem s must have the same displacement, that is $u_l^{(r)} - u_m^{(s)} = 0$.

This condition can be generally expressed as:

$$\mathbf{B}\boldsymbol{u} = \mathbf{0} \tag{3}$$

where each row of $\mathbf{B}$ corresponds to a pair of matching DoFs.

The equilibrium condition for internal constraint forces implies that, when the connecting forces are considered at a pair of matching DoFs, their sum must be zero, i.e. $g_l^{(r)} + g_m^{(s)} = 0$: this holds for any pair of matching DoFs. Furthermore, if DoF k on subsystem q is not a connecting DoF, it must be $g_k^{(q)} = 0$: this holds for any non-interface DoF.

Overall, the above conditions can be expressed as:

$$\mathbf{L}^T\boldsymbol{g} = \mathbf{0} \tag{4}$$

where the matrix $\mathbf{L}$ is a Boolean localisation matrix.

Eqs. (2-4) can be put together to obtain the so-called three-field formulation, describing the coupling between any number of subsystems:

$$\begin{cases} \mathbf{Z}\boldsymbol{u} = \boldsymbol{f} + \boldsymbol{g} \\ \mathbf{B}\boldsymbol{u} = \mathbf{0} \\ \mathbf{L}^T\boldsymbol{g} = \mathbf{0} \end{cases} \tag{5}$$

In the dual formulation [15, 22], the total set of DoFs is retained, i.e. each interface DoF is present as many times as there are substructures connected through that DoF. The equilibrium condition $g_l^{(r)} + g_m^{(s)} = 0$ at a pair of interface DoFs is ensured by choosing, for instance, $g_l^{(r)} = -\lambda$ and $g_m^{(s)} = \lambda$. Therefore, the equilibrium of internal constraint forces can be ensured by writing the connecting forces in the form:

$$\boldsymbol{g} = -\mathbf{B}^T\boldsymbol{\lambda} \tag{6}$$

where $\boldsymbol{\lambda}$ are Lagrange multipliers corresponding to connecting force intensities.

The equilibrium of internal constraint forces (4) is thus written:

$$\mathbf{L}^T\boldsymbol{g} = -\mathbf{L}^T\mathbf{B}^T\boldsymbol{\lambda} = \mathbf{0} \qquad \forall\boldsymbol{\lambda} \tag{7}$$

Since Eq. (7) is always satisfied by any set of connecting force intensities $\boldsymbol{\lambda}$, the system of equations (5) becomes:

$$\begin{cases} \mathbf{Z}\boldsymbol{u} + \mathbf{B}^T\boldsymbol{\lambda} = \boldsymbol{f} \\ \mathbf{B}\boldsymbol{u} = \mathbf{0} \end{cases} \tag{8}$$

To eliminate $\boldsymbol{\lambda}$, from the first of Eq. (8), it can be written:

$$\boldsymbol{u} = -\mathbf{Z}^{-1}\mathbf{B}^T\boldsymbol{\lambda} + \mathbf{Z}^{-1}\boldsymbol{f} \tag{9}$$

which substituted in the second of Eq. (8) gives:

$$\mathbf{B}\mathbf{Z}^{-1}\mathbf{B}^T\boldsymbol{\lambda} = \mathbf{B}\mathbf{Z}^{-1}\boldsymbol{f} \quad \Rightarrow \quad \boldsymbol{\lambda} = \left(\mathbf{B}\mathbf{Z}^{-1}\mathbf{B}^T\right)^{-1}\mathbf{B}\mathbf{Z}^{-1}\boldsymbol{f} \tag{10}$$

Substituting $\boldsymbol{\lambda}$ in the first of Eq. (8), it is obtained:

$$\begin{aligned} &\mathbf{Z}\boldsymbol{u} + \mathbf{B}^T\left(\mathbf{B}\mathbf{Z}^{-1}\mathbf{B}^T\right)^{-1}\mathbf{B}\mathbf{Z}^{-1}\boldsymbol{f} = \boldsymbol{f} \\ \Rightarrow \qquad &\boldsymbol{u} = \left(\mathbf{Z}^{-1} - \mathbf{Z}^{-1}\mathbf{B}^T\left(\mathbf{B}\mathbf{Z}^{-1}\mathbf{B}^T\right)^{-1}\mathbf{B}\mathbf{Z}^{-1}\right)\boldsymbol{f} \end{aligned} \tag{11}$$

By considering that:

$$\mathbf{Z}^{-1} = \mathbf{H} = \begin{bmatrix} \mathbf{H}^{(1)} & & \\ & \ddots & \\ & & \mathbf{H}^{(n)} \end{bmatrix} \tag{12}$$

being $\mathbf{H}^{(r)} = [\mathbf{Z}^{(r)}]^{-1}$ the Frequency Response Function (FRF) matrix of the r-th subsystem, Eq. (11) can be rewritten:

$$\boldsymbol{u} = \left(\mathbf{H} - \mathbf{H}\mathbf{B}^T \left(\mathbf{B}\mathbf{H}\mathbf{B}^T \right)^{-1} \mathbf{B}\mathbf{H} \right) \boldsymbol{f} \tag{13}$$

Therefore, by considering that the FRF matrix $\mathbf{H}_c$ of the coupled system satisfies the relation $\boldsymbol{u} = \mathbf{H}_c \boldsymbol{f}$, it is:

$$\mathbf{H}_c = \mathbf{H} - \mathbf{H}\mathbf{B}^T \left(\mathbf{B}\mathbf{H}\mathbf{B}^T \right)^{-1} \mathbf{B}\mathbf{H} \tag{14}$$

Note that the rows and columns corresponding to the coupling DoFs appear twice in $\mathbf{H}_c$. Obviously, only independent entries are retained.

Configuration Dependent Interface An interesting extension of the substructuring approach is to consider systems built from time-invariant component subsystems subjected to configuration dependent coupling conditions, such as those encountered when a relative motion exists between two coupled bodies.

In this case, compatibility and equilibrium conditions become configuration dependent. If χ denotes a given configuration, the compatibility condition can be generally expressed as:

$$\mathbf{B}_\mathbf{C}(\chi)\boldsymbol{u}(\chi) = \mathbf{0} \tag{15}$$

where each row of $\mathbf{B}_\mathbf{C}(\chi)$ concerns a pair of matching DoFs at configuration χ.

The equilibrium condition $g_l^{(r)}(\chi) + g_m^{(s)}(\chi) = 0$ at a pair of interface DoFs is ensured by choosing, for instance, $g_l^{(r)}(\chi) = -\lambda(\chi)$ and $g_m^{(s)}(\chi) = \lambda(\chi)$. Therefore, the overall interface equilibrium can be ensured by writing the connecting forces in the form:

$$\boldsymbol{g}(\chi) = -{\mathbf{B}_\mathbf{E}}^T(\chi)\boldsymbol{\lambda}(\chi) \tag{16}$$

where $\boldsymbol{\lambda}(\chi)$ are Lagrange multipliers corresponding to connecting force intensities and $\mathbf{B}_\mathbf{E}(\chi)$ is different from the signed Boolean matrix $\mathbf{B}_\mathbf{C}(\chi)$ used to enforce the compatibility condition, because $\mathbf{B}_\mathbf{E}(\chi)$ must also account for friction forces at the interface.

2.2 Configuration dependent frequency response function

A configuration dependent frequency response function of the coupled system can be computed as follows. When a configuration dependent interface is considered, Eq. (8) can be rewritten as:

$$\begin{cases} \mathbf{Z}\boldsymbol{u}(\chi) + {\mathbf{B}_\mathbf{E}}^T(\chi)\boldsymbol{\lambda}(\chi) = \boldsymbol{f} \\ \mathbf{B}_\mathbf{C}(\chi)\boldsymbol{u}(\chi) = \mathbf{0} \end{cases} \tag{17}$$

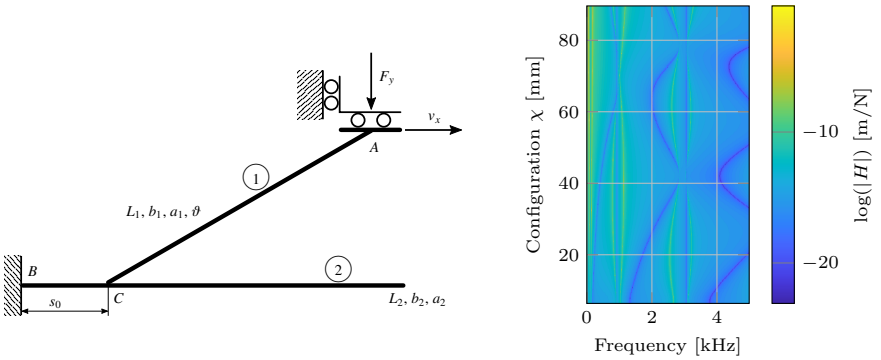

(a) Beam on beam model [3]. (b) $|H_{CyCy}(\omega, \chi)|$.

Fig. 1: Configuration dependent beam on beam model.

A procedure similar to that outlined in Eqs. (9)-(13) can be followed to eliminate $\lambda(\chi)$ from the first of Eq. (17) and to obtain, finally, an expression of the FRF matrix of the coupled system with configuration dependent interface:

$$\mathbf{H}_c(\chi) = \mathbf{H} - \mathbf{H}\mathbf{B}_\mathbf{E}{}^T(\chi) \left(\mathbf{B}_\mathbf{C}(\chi)\mathbf{H}\mathbf{B}_\mathbf{E}{}^T(\chi)\right)^{-1} \mathbf{B}_\mathbf{C}(\chi)\mathbf{H} \tag{18}$$

In Fig. 1a, a beam on beam system is considered, where the upper oblique beam 1 is subjected to a vertical load F_y and to a constant velocity v_x in the horizontal direction. Therefore, the contact point C moves from the fixed end to the free end of the horizontal beam. More details about the system characteristics are available in [3]. Fig. 1b shows the configuration dependent drive point FRF at the contact point C, computed according to Eq. (18). It can be noticed that the low level pattern highlights configuration dependent anti-resonance locations, while the high level pattern accounts for configuration dependent resonance location.

3 Decoupling

As stated in the Introduction, substructure decoupling consists in the identification of a dynamic model of a structural subsystem, starting from the FRFs of the assembled system RU and from a dynamic model of the so-called residual subsystem R. The unknown subsystem U (N_U DoFs) is joined to the residual subsystem R (N_R DoFs) by n_c coupling DoFs through which constraint forces (and moments) are exchanged (see Fig. 2). The degrees of freedom of the assembled structure (N_{RU} DoFs) can be partitioned into coupling DoFs (c), internal DoFs of substructure U (u) and internal DoFs of substructure R (r).

The FRFs of the unknown substructure U can be predicted from those of the assembled structure RU by taking out the dynamic effect of the residual subsystem R. In principle, this can be accomplished by considering a negative structure, i.e. by adding to the assembled structure RU a fictitious substructure

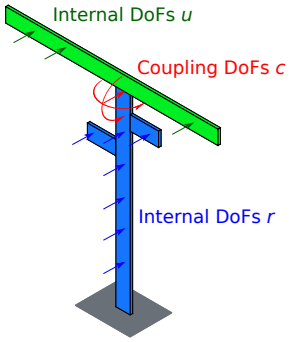

Fig. 2: Assembled system RU, with the unknown subsystem U (green) and the residual subsystem R (blue) [11]. (For interpretation of the references to colour in the text, the reader is referred to the web version of this chapter.)

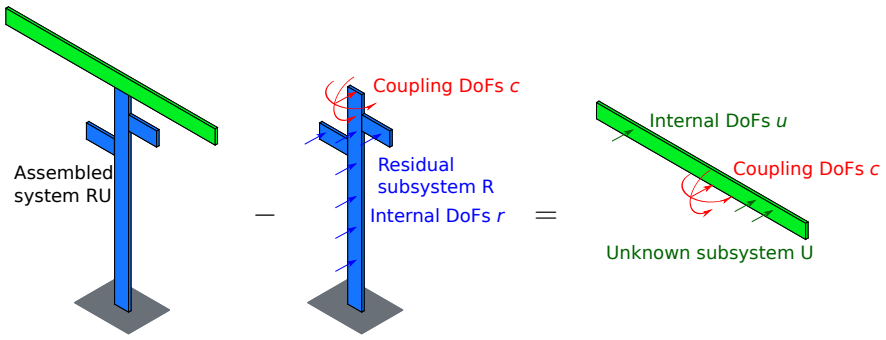

Fig. 3: Scheme of the direct decoupling problem [11].

with a dynamic stiffness opposite to that of the residual substructure R (see Fig. 3). The effect of the negative structure is to add a set of disconnection forces (and moments) to the external forces acting on the assembled system in order to uncouple the unknown substructure from the assembled structure. However, the set of disconnection forces is not unique. In fact, several sets of disconnection forces can be devised:

- a trivial set, consisting of disconnection forces acting at the coupling DoFs and opposite to the constraint forces (see Fig. 4); in this case, disconnection forces may include moments opposite to the constraint moments.
- non trivial sets of disconnection forces acting at different DoFs but able to cancel the constraint forces at the coupling DoFs (see Fig. 5); in this case, disconnection forces applied to internal DoFs must be able to provide a moment about the rotation axes.

In both cases, the dynamic equilibrium of the assembled structure RU is:

$$\mathbf{Z}^{\mathbf{RU}}\boldsymbol{u}^{\boldsymbol{RU}} = \boldsymbol{f}^{\boldsymbol{RU}} + \boldsymbol{g}^{\boldsymbol{RU}} \tag{19}$$

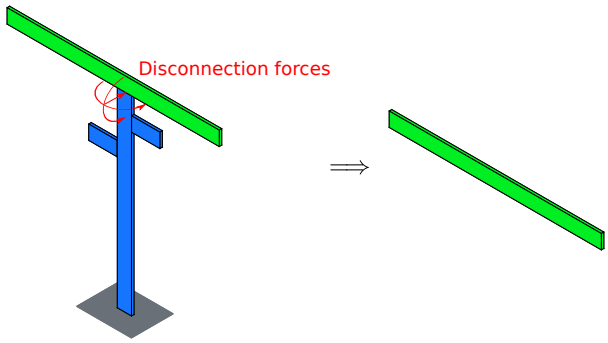

Fig. 4: Trivial set of disconnection forces (and moments) acting on the assembled structure (corresponding to the standard interface) [11].

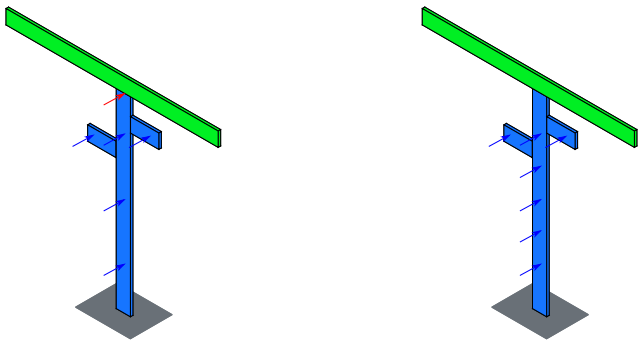

Fig. 5: Non trivial sets of disconnection forces corresponding to a mixed interface (left) and to a pseudo interface (right) [11].

where $\boldsymbol{g}^{\boldsymbol{RU}}$ is the vector of disconnection forces applied to the assembled structure by the negative structure, $\mathbf{Z}^{\mathbf{RU}}$ is the dynamic stiffness matrix of the assembled structure RU, $\boldsymbol{u}^{\boldsymbol{RU}}$ is the vector of degrees of freedom of the assembled structure RU, $\boldsymbol{f}^{\boldsymbol{RU}}$ is the external force vector on the assembled structure RU.

Similarly, the dynamic equilibrium of the negative structure is expressed as:

$$-\mathbf{Z}^{\mathbf{R}}\boldsymbol{u}^{\boldsymbol{R}} = \boldsymbol{f}^{\boldsymbol{R}} + \boldsymbol{g}^{\boldsymbol{R}} \tag{20}$$

where $-\mathbf{Z}^{\mathbf{R}}$ is the dynamic stiffness matrix of the negative structure, and $\boldsymbol{u}^{\boldsymbol{R}}$, $\boldsymbol{f}^{\boldsymbol{R}}$ and $\boldsymbol{g}^{\boldsymbol{R}}$ are defined as for the assembled structure.

In order that Eqs. (19-20) can be put together to represent the unknown substructure U, disconnection forces $\boldsymbol{g}^{\boldsymbol{RU}}$ and $\boldsymbol{g}^{\boldsymbol{R}}$ must be in equilibrium, and compatibility between degrees of freedom $\boldsymbol{u}^{\boldsymbol{RU}}$ and $\boldsymbol{u}^{\boldsymbol{R}}$ must hold at the interface between the assembled structure RU and the negative structure. Note that such interface includes both the coupling DoFs between substructures U and R, and the internal DoFs of substructure R (the blue part of the structure in Fig. 3). However, it is not necessary to retain the full set of these interface DoFs,

because it is sufficient that the number of interface DoFs be not less than the number of coupling DoFs n_c. Therefore, several options for interface DoFs can be considered:

- standard interface, including only the coupling DoFs (c) between substructures U and R, e.g. those corresponding to the disconnection forces (and moments) in Fig. 4;
- extended interface, including also a subset of internal DoFs ($i \subseteq r$) of substructure R;
- mixed interface, including subsets of coupling ($d \subset c$) and internal DoFs ($i \subseteq r$), e.g. those corresponding to the disconnection forces in Fig. 5 (left);
- pseudo interface, including only internal DoFs ($i \subseteq r$) of substructure R, e.g. those corresponding to the disconnection forces in Fig. 5 (right).

The use of a mixed or pseudo interface allows to replace rotational coupling DoFs with translational internal DoFs.

Compatibility at the (standard, extended, mixed, pseudo) interface implies that any pair of matching DoFs, i.e. DoF l on the coupled system RU and DoF m on subsystem R, must have the same displacement, that is $u_l^{RU} - u_m^R = 0$. Let S_C be the set of N_C interface DoFs on which compatibility is enforced. The compatibility condition can be expressed as:

$$\mathbf{B_C}\,\boldsymbol{u} = 0 \qquad \text{where:} \quad \boldsymbol{u} = \begin{Bmatrix} \boldsymbol{u^{RU}} \\ \boldsymbol{u^{R}} \end{Bmatrix} \tag{21}$$

where $\mathbf{B_C}$ has size $N_C \times (N_{RU} + N_R)$ and each row corresponds to a pair of matching DoFs.

Let S_E be the set of N_E interface DoFs on which equilibrium is enforced. Note that sets S_E and S_C can be different (non-collocated approach [22]); the traditional approach, when $S_E \equiv S_C$, is called collocated. The equilibrium of disconnection forces implies that for any pair of matching DoFs, i.e. DoF r on the coupled system RU and DoF s on subsystem R, their sum must be zero, that is $g_r^{RU} + g_s^R = 0$. In the dual assembly, the total set of DoFs is retained, and the equilibrium at a pair of matching DoFs is ensured by choosing $g_r^{RU} = -\lambda_r$ and $g_s^R = \lambda_r$. Therefore, the overall interface equilibrium can be ensured by writing the disconnection forces in the form:

$$\boldsymbol{g} = -\mathbf{B_E}^T\,\boldsymbol{\lambda} \qquad \text{where:} \quad \boldsymbol{g} = \begin{Bmatrix} \boldsymbol{g^{RU}} \\ \boldsymbol{g^{R}} \end{Bmatrix} \tag{22}$$

where $\boldsymbol{\lambda}$ is a vector of Lagrange multipliers corresponding to disconnection force intensities, and $\mathbf{B_E}$ is a $N_E \times (N_{RU} + N_R)$ matrix.

Having defined $\mathbf{B_C}$ and $\mathbf{B_E}$, an expression of the FRF $\mathbf{H^U}$ of the unknown subsystem can be derived using the same procedure as in section 2.2, leading to:

$$\mathbf{H^U} = \mathbf{H} - \mathbf{H}\mathbf{B_E}^T \left(\mathbf{B_C}\mathbf{H}\mathbf{B_E}^T\right)^+ \mathbf{B_C}\mathbf{H} \tag{23}$$

where + denotes the pseudo-inverse. This operation is necessary because it can be $N_C \neq N_E$. To obtain a determined or overdetermined matrix for the generalized inversion operation, the number of rows of $\mathbf{B_C}$ must be greater or equal than the number of rows of $\mathbf{B_E}$, i.e.

$$N_C \geq N_E \geq n_c \tag{24}$$

3.1 Interface Optimization

Disconnection forces $\boldsymbol{g}^{RU}$ must be able to uncouple the unknown substructure from the assembled system, i.e. they are such as to cancel constraint forces at the coupling DoFs. If coupling DoFs include rotational DoFs, constraint forces include moments about some given axes.

As stated at the beginning of section 3, the set of disconnection forces is not unique. Therefore, non trivial sets of disconnection forces, typically not including moments, can be selected taking into account the further objective of avoiding ill conditioning problems.

In Eq. (23), the product $\mathbf{B_C H B_E}^T$ that has to be inverted is defined as interface flexibility matrix. In fact, as shown in [9], it can be rewritten as:

$$\mathbf{B_C H B_E}^T = \hat{\mathbf{H}}^{\mathbf{RU}} - \hat{\mathbf{H}}^{\mathbf{R}} \tag{25}$$

where $\hat{\mathbf{H}}^{\mathbf{RU}}$ and $\hat{\mathbf{H}}^{\mathbf{R}}$ are the FRFs of the assembled structure and of the residual substructure at interface DoFs. The interface flexibility matrix depends on the choice of interface DoFs and it can be ill conditioned for some set of interface DoFs. Therefore, the conditioning of the interface flexibility matrix must be taken into account in the choice of interface DoFs.

An application is performed on the assembled system shown in Fig. 6a. The residual subsystem R consists of a cantilever beam with two offset short arms (Fig. 6b). The unknown substructure U is the beam bolted to the free end of the cantilever beam. The joint involves both translational and rotational DoFs. More details are available in [10].

The experimental FRF matrix of the assembled system is obtained at seven locations (3, 6, 9, 10, 11, 13, 20) along the z-direction orthogonal to the plane of the structure. For the residual subsystem, the experimental FRF matrix is similarly measured at five locations (3, 6, 9, 10, 11). Coupling DoFs are: $11z$, $11\theta_x$ and $11\theta_y$, that is one translational DoF and two rotational DoFs around the horizontal and vertical directions in the plane of the structure.

There are 3 coupling DoFs, so that $n_c = 3$. As stated in Eq. (24), it must be $N_E \geq n_c = 3$, where $n_c = 3$ is the minimal number of DoFs. Therefore, in principle, any set of at least 3 DoFs among the measured DoFs on the residual subsystem is a possible set of interface DoFs. It can be quite significant to compare minimal sets of DoFs.

As shown in [10], either DoF $9z$ or DoF $10z$ must be included among the interface DoFs so that the corresponding disconnection force is able to provide a moment around DoF $11\vartheta_y$. The objective is to select, between DoFs $9z$ and $10z$,

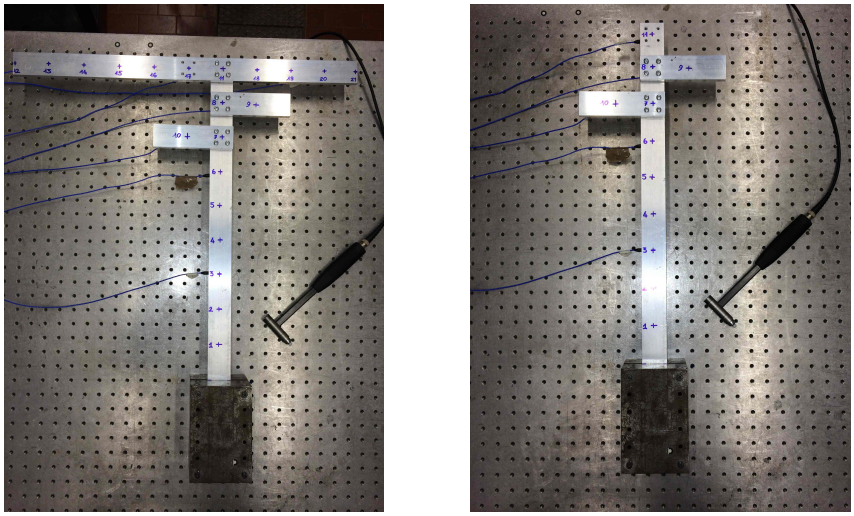

(a) Assembled system. (b) Residual subsystem.

Fig. 6: Experimental test bed for decoupling [11].

the most appropriate in terms of the condition number of the interface flexibility matrix. It may be convenient, although not strictly necessary, to keep one of the coupling DoFs, in this case DoF $11z$, among the interface DoFs.

Therefore, two minimal sets of DoFs are compared, each one of then representing a mixed interface: $11z$, $3z$, $9z$ and $11z$, $3z$, $10z$.

The condition number of the interface flexibility matrix $\hat{\mathbf{H}}^{\mathbf{RU}} - \hat{\mathbf{H}}^{\mathbf{R}}$ is considered for each of the two sets of interface DoFs (Fig. 7). It can be noticed that the condition number is lower when DoF $9z$ is considered instead of DoF $10z$, except in a limited frequency range, i.e. 1200-1300 Hz. Therefore, according to this criterion, DoF $9z$ should be preferred to DoF $10z$.

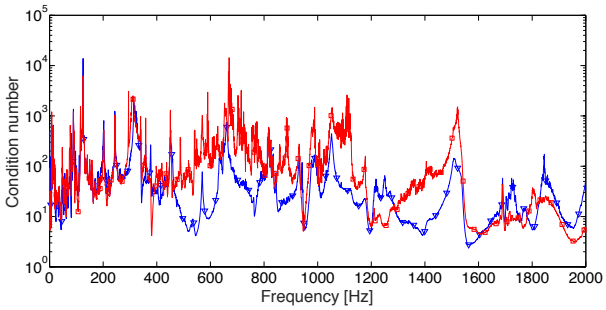

Fig. 7: Condition number of the interface flexibility matrix using experimental data and interface DoFs : $11z$, $3z$, $9z$ (–▽–); $11z$, $3z$, $10z$ (–□–) [10].

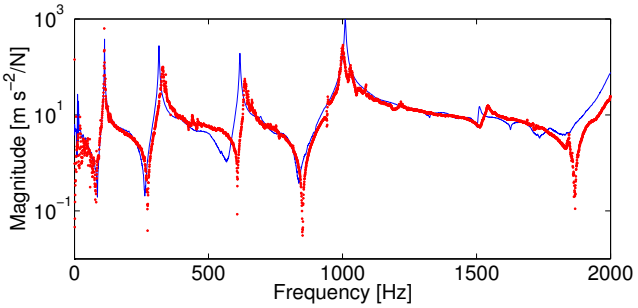

Fig. 8: $H^U_{11z,11z}$: measured (—), predicted from experimental FRFs using coupling DoF $11z$ and internal DoFs $3z$, $9z$ (***) [10].

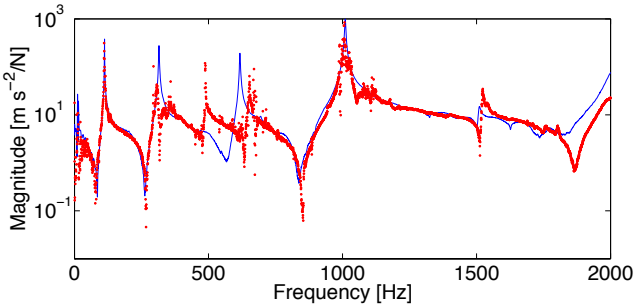

Fig. 9: $H^U_{11z,11z}$: measured (—), predicted from experimental FRFs using coupling DoF $11z$ and internal DoFs $3z$, $10z$ (***) [10].

FRFs of the unknown substructure are predicted using the two sets of minimal interface DoFs defined previously. To check decoupling results, FRFs are measured also at three locations (11, 13, 20) of the unknown subsystem U. The FRF of the unknown substructure U, predicted using interface DoFs $11z$, $3z$, $9z$, is shown in Fig. 8: the result is quite clean considering that experimental data are being used. The FRF of the unknown substructure U, predicted using interface DoFs $11z$, $3z$, $10z$, is shown in Fig. 9: the result is much worse than in the previous case, especially in the frequency band 400-1000 Hz, where the condition number of the interface flexibility matrix using interface DoFs $11z$, $3z$, $9z$ is significantly lower than using interface DoFs $11z$, $3z$, $10z$.

4 Perspectives

Perspectives of experimental dynamic substructuring differ according to whether substructure coupling problems or substructure decoupling problems are considered. With reference to substructure coupling problems, the most promising fields are those of coupling with configuration dependent interface and of nonlinear coupling with localized nonlinearities.

Coupling with configuration dependent interface is discussed in section 2.1 and a simple example of configuration dependent Frequency Response Function is shown in section 2.2: the example considers numerically simulated FRFs, but the procedure can be readily extended to experimental FRFs.

Nonlinear coupling with localized nonlinearities, i.e. linear structures connected by nonlinear joints is an ongoing field of research. The focus is about the effects of nonlinear connections on the dynamics of an assembly in which the coupled subsystems can be assumed as linear. This is suitable in many engineering systems where the nonlinearity introduced by the connecting element is much more relevant than those of the substructures to be coupled, as for bolted joints, wire rope isolators, turbine blade-rotor connections, etc. The advantages of nonlinear dynamic substructuring, where the nonlinear connecting elements are modeled using nonlinear normal modes, are shown in several papers [17, 16].

The most remarkable topics in substructure decoupling are: interface optimization and disconnection force identification; decoupling with configuration dependent coupling conditions; joint identification, including nonlinear joints.

Interface optimization, discussed in section 3.1, concerns how to select the best set of DoFs in order to have a good conditioning of the interface flexibility matrix. In fact, by considering pseudo-interfaces, measurements on the connecting DoFs can be avoided. This is useful when for instance connecting DoFs are difficult to access. Identification of disconnection forces is discussed in [11].

Substructure decoupling with configuration dependent coupling conditions is a very challenging task, that can lead to interesting results for instance when only the coupling conditions are configuration dependent, while the subsystems to be coupled are not, as for a lifting crane or a Cartesian robot.

Among the many techniques that can be devised to deal with joint identification, substructure decoupling is - in the authors' opinion – one of the most promising. Typically, the envisaged process involves subsequent steps of substructure coupling and decoupling: model mixing techniques [14, 19] can be used to merge experimental measurements and theoretical models, and nonlinear joints can be identified by experimentally varying the excitation level [13].

References

1. Bello, M., Sestieri, A., D'Ambrogio, W., La Gala, F.: Development of a rotational transducer based on bimorph PZT's. Mechanical Systems and Signal Processing **17**(5), 1069–1081 (Sep 2003)
2. Brunetti, J., D'Ambrogio, W., Fregolent, A.: Contact problems in the framework of dynamic substructuring. In: Moens, D., Desmet, W., Pluymers, B., Rottiers, W. (eds.) Proceedings of ISMA 2018 and USD 2018, pp. 3987–3998. KU Leuven - Dept. Werktuigkunde (2018)
3. Brunetti, J., D'Ambrogio, W., Fregolent, A.: Dynamic coupling of substructures with sliding friction interfaces. Mechanical Systems and Signal Processing **141**, 106731 (2020)
4. Brunetti, J., D'Ambrogio, W., Fregolent, A.: Dynamic substructuring with time variant coupling conditions for the analysis of friction induced vibrations. In:

Desmet, W., Pluymers, B., Moens, D., Vandemaele, S. (eds.) Proceedings of ISMA 2020 and USD 2020, pp. 3023–3032. KU Leuven - Dept. Werktuigkunde (2020)
5. Brunetti, J., D'Ambrogio, W., Fregolent, A.: Friction-induced vibrations in the framework of dynamic substructuring. Nonlinear Dynamics **103**(4), 3301–3314 (2021)
6. Brunetti, J., D'Ambrogio, W., Fregolent, A.: Dynamic substructuring with a sliding contact interface. In: Linderholt, A., Allen, M.S., Mayes, R.L., Rixen, D. (eds.) Dynamics of Coupled Structures, Volume 4, pp. 105–116. Springer International Publishing (2018). https://doi.org/10.1007/978-3-319-74654-8_9
7. Brunetti, J., D'Ambrogio, W., Fregolent, A.: Dynamic substructuring with time variant interface due to sliding friction. In: Carcaterra, A., Paolone, A., Graziani, G. (eds.) Proceedings of XXIV AIMETA Conference 2019, pp. 1459–1474. Springer International Publishing (2020). https://doi.org/10.1007/978-3-030-41057-5_118
8. Craig, R., Bampton, M.: Coupling of substructures for dynamic analyses. AIAA Journal **6**(7), 1313–1319 (1968)
9. D'Ambrogio, W., Fregolent, A.: Substructure decoupling without using rotational dofs: Fact or fiction? Mechanical Systems and Signal Processing **72-73**, 499–512 (2016)
10. D'Ambrogio, W., Fregolent, A.: Replacement of unobservable coupling dofs in substructure decoupling. Mechanical Systems and Signal Processing **95**, 380–396 (2017)
11. D'Ambrogio, W., Fregolent, A.: Substructure decoupling as the identification of a set of disconnection forces. Meccanica **52**(13), 3117–3129 (2017)
12. Hurty, W.: Dynamic analysis of structural systems using component modes. AIAA Journal **3**(4), 678–685 (1965)
13. Kalaycioglu, T., Ozguven, H.: Frf decoupling of nonlinear systems. Mechanical Systems and Signal Processing **102**, 230–244 (2018)
14. Klaassen, S., van der Seijs, M., de Klerk, D.: System equivalent model mixing. Mechanical Systems and Signal Processing **105**, 90–112 (2018)
15. de Klerk, D., Rixen, D.J., Voormeeren, S.: General framework for dynamic substructuring: History, review, and classification of techniques. AIAA Journal **46**(5), 1169–1181 (2008)
16. Latini, F., Brunetti, J., D'Ambrogio, W., Allen, M., Fregolent, A.: Nonlinear substructuring in the modal domain: numerical validation and experimental verification in presence of localized nonlinearities. Nonlinear Dynamics **104**(2), 1043–1067 (2021)
17. Latini, F., Brunetti, J., D'Ambrogio, W., Fregolent, A.: Substructures' coupling with nonlinear connecting elements. Nonlinear Dynamics **99**(2), 1643–1658 (2020)
18. Rubin, S.: Improved component-mode representation for structural dynamic analysis. AIAA Journal **13**(8), 995–1006 (1975)
19. Saeed, Z., Klaassen, S., Firrone, C., Berruti, T., Rixen, D.: Experimental joint identification using system equivalent model mixing in a bladed disk. Journal of Vibration and Acoustics, Transactions of the ASME **142**(5), 051001 (2020)
20. Sestieri, A., Salvini, P., D'Ambrogio, W.: Reducing scatter from derived rotational data to determine the frequency response function of connected structures. Mechanical Systems and Signal Processing **5**(1), 25–44 (1991)
21. Stanbridge, A., Ewins, D.: Measurement of translational and angular vibration using a scanning laser doppler vibrometer. Shock and Vibration **3**, 141–152 (1996)
22. Voormeeren, S.N., Rixen, D.J.: A family of substructure decoupling techniques based on a dual assembly approach. Mechanical Systems and Signal Processing **27**, 379–396 (2012)